Molecular Dynamics Applied to Nucleic Acids

JAN NORBERG*,† AND LENNART NILSSON*,‡

Center for Structural Biochemistry, Department of Biosciences at Novum Karolinska Institutet, S-141 57 Huddinge, Sweden

Received November 14, 2001

ABSTRACT

In this Account, we focus on molecular dynamics (MD) simulations involving fully solvated nucleic acids. Historically, MD simulations were first applied to proteins and several years later to nucleic acids. The first MD simulations of DNA were carried out in vacuo, but nowadays fully solvated systems are common practice. Recently, technical improvements have made it possible to conduct accurate MD simulations of highly charged nucleic acids. The state-of-the-art of MD simulations and a number of applications on various nucleic acid systems are discussed.

Introduction

It is now 25 years since the first molecular dynamics (MD) simulation of a biological macromolecule was published.[1] The first MD studies focused on the bovine pancreatic trypsin inhibitor protein and were carried out in vacuo. It took several years until the first MD simulations of nucleic acid systems were performed.[2−6] These investigations, which were also performed in vacuo, clearly demonstrated the importance of proper handling of electrostatics in a highly charged nucleic acid system, and different approaches, such as reduction of the phosphate charges and addition of hydrated counterions, have been applied to remedy this shortcoming and to maintain stable DNA structures. A few years later, the first MD simulation of a DNA molecule, including explicit water molecules and counterions, was published.[7] Nowadays, this is common practice, and MD simulations of nucleic acids have become abundant.[8−11] Much of this has arisen from accurate parametrization of the nucleic acids force fields[12,13] but also from algorithmic development. In this Account, we discuss a few specific topics concerning MD simulations of DNA duplexes and some RNA molecules. Because of space limitations, the selection is somewhat subjective, but we believe that these studies demonstrate the feasibility of MD simulations of nucleic acid systems. The maturity of the field is further indicated by the substantial body of recent literature[10,11] on applications of MD methods to a variety of systems, including nucleic acids and biomolecular complexes containing nucleic acids[14−22] that are not covered here: Z-DNA, triplexes, quadruplexes, drug−DNA complexes, and the effects of base and backbone modifications.

Base Stacking in Single-Stranded Oligonucleotides

Base stacking is one of the driving forces for DNA folding and stability. Unlike hydrogen-bonded base pairing, base stacking is sequence-dependent, and it is, therefore, a key feature in nucleic acid secondary structure formation. To fully understand the base stacking phenomenon, it is advantageous to focus on nucleic acid fragments in solution. For instance, base stacking has been investigated by performing MD simulations of stacked and unstacked conformations of the dinucleotide GpU[23] at atmospheric pressure and at higher pressures, 5000 atm and 12 000 atm,[24] yielding results in agreement with experimental data[25] on nucleic acid conformations at elevated pressures. The all-atom root-mean-square deviations (RMSD) from the X-ray crystal structure were between 0.8 and 1.3 Å, demonstrating the accuracy in the MD simulations. These values are very similar to results obtained for RNA dinucleotides using the particle mesh Ewald algorithm to handle the electrostatic interactions in which heavy-atom RMSD values of 0.4 and 1.02 Å were found in crystal environment and in solution, respectively.[26] To further investigate the thermodynamics of stacking, free energy surfaces of all the naturally occurring DNA and RNA dinucleotides have been determined.[27,28] In these potential of mean force calculations, the transition from a stacked conformation to an unstacked form was monitored using the distance between the glycosidic nitrogen atoms of the bases as the reaction coordinate. The base stacking preferences were found to follow the general sequence purine−purine > purine−pyrimidine ≥ pyrimidine−purine > pyrimidine−pyrimidine. DNA dimers composed of at least one purine base showed good stacking, with the unstacked states ≥2 kcal/mol higher in energy than the stacked. During the unstacking process, the purines remain parallel until they are sufficiently far apart to be individually solvated (Figure 1), whereas the pyrimidine bases, except thymidine, rotate more freely, even in the stacked conformation. For pyrimidines, significant stacking propensities were, therefore, found for dimers containing a thymine base and a purine base and also for the dTdT dimer. Furthermore, the free energy barrier for unstacking of ApA was found to decrease with increasing temperature,[29] and the entropy and enthalpy components calculated from this temperature dependence were in good agreement with experimental data.

Dr. Jan Norberg is a researcher at the Department of Biosciences, Karolinska Institutet in Stockholm, Sweden. He received his Ph.D. in 1995 in structural biochemistry.

Lennart Nilsson is Professor of molecular modeling at the Department of Biosciences, Karolinska Institutet, Stockholm, Sweden. He was born in 1952 in Stockholm, Sweden, and received his degree in physics from the Royal Institute of Technology in 1976. After obtaining his Ph.D. in 1983 in theoretical physics and a postdoctoral period at Harvard University, he returned to Karolinska Institutet in 1985. His current research interests are in nucleic acid−protein interactions and nucleic acid structural dynamics.

† Telephone: +46 8 608 9264. E-mail: Jan.Norberg@biosci.ki.se.

‡ Telephone: +46 8 608 9228. Fax: +46 8 608 9290. E-mail: Lennart.Nilsson@biosci.ki.se.

10.1021/ar010026a CCC: $22.00
Published on Web 04/26/2002

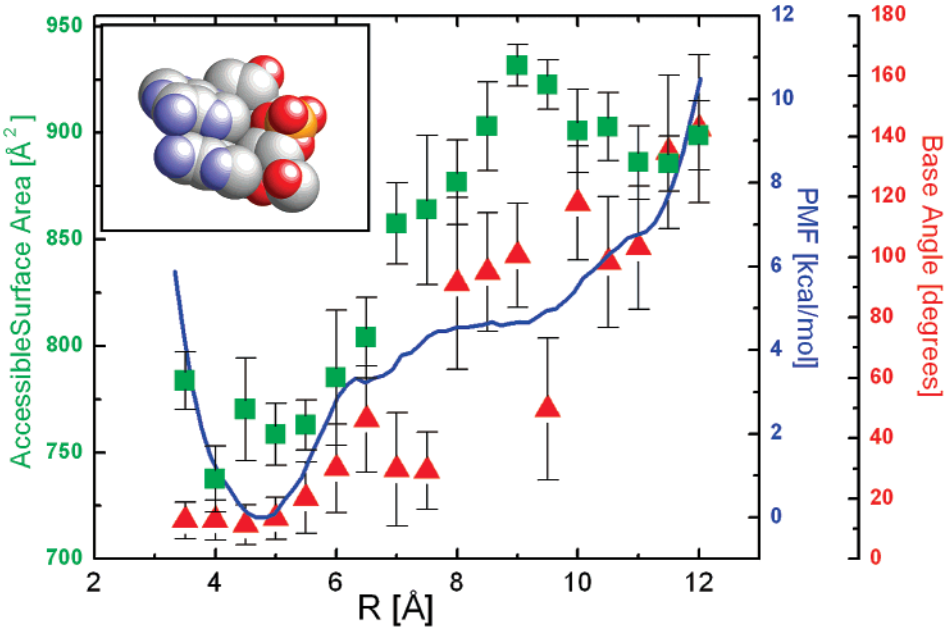

FIGURE 1. Free energy surface of the ApA dimer (—), base−base angle (▲), and accessible surface area (■) versus the reaction coordinate. Inset: ApA in stacked conformation with A-RNA geometry.

Other factors that may be important for stacking are the backbone,[27,28,30,31] bases further away,[32,33] and the solvent.[34] In simulations of a thymidine dimer with a neutral methylene methyl imino backbone,[30] the backbone showed several conformational transitions, and two populations of low energy conformations with preserved base stacking were observed. In the case of GpN vs GpNp, a different situation was found. Barnase has low catalytic activity toward GpN dinucleotides but significantly larger for GpNp. This has been investigated by MD simulations of GpA and GpAp in aqueous solution,[31] in which the GpA dimer showed a large propensity for a folded conformation with the bases stacked, but the GpAp mainly remained unfolded. A hydrogen bond between the terminal phosphate and the adenosine ribose group was the main reason for the extended structure. The neighboring bases influence the stacking ability to some degree, even though the main determinant is the nature of the two bases directly involved. Conformational free energy landscapes of the trinucleotide ApApA[32] and of several tetramers[33] have been determined from potential of mean force calculations, and it was found that flanking purines enhance the stacking of two bases, in particular for the case in which the two central bases in a tetramer are pyrimidines. A comparison of the stacking free energy of a DNA and an RNA dimer in organic solvents and in aqueous solution shows the stacking ability to be greater in aqueous solution than in low dielectric solvents, such as chloroform.[34]

The simulation data, thus, show that nucleotide stacking is an enthalpy-driven process dominated by nearest-neighbor interactions, more pronounced in aqueous solution than in low-dielectric organic solvents, and it is more favorable for purines than for the smaller pyrimidines, which can easily become independently solvated, even when they are close in space.

A- and B-DNA

The most studied nucleic acid structure both experimentally and theoretically is the dodecamer d(CGCGAATTCGCG)$_2$, which contains the GAATTC tract that is the recognition site for the restriction enzyme EcoRI endonuclease. One of the first MD simulation studies of a nucleic acid investigated this dodecamer in vacuo,[2] and shortly after that, the first MD simulation including counterions and explicit water molecules of a five-base-pair DNA duplex was reported.[7] Since then, a large number of both in vacuo and solution MD reports have been published[8−11] with a very clear trend toward simulations in explicit solvent. A recent X-ray crystallographic determination[35] of the structure of d(CATCCCGGGATG)$_2$ shows it to be intermediate between the A and B forms (Figure 2). Judging from the RMSD, it is slightly closer to the A form, in particular if the bases of the middle six base pairs are compared (Table 1). For comparison, Table 1 also shows that the EcoRI dodecamer[36] is much closer to the B form. The transition between the A and B forms of DNA appears to be gradual,[35,37] and thus, it is a nontrivial task to get this equilibrium and its dependence on environment and sequence from simulations. Here, we focus on only a few very recently published investigations.

The EcoRI dodecamer and two other DNA 25-mer oligonucleotides were very stable in up to 15-ns-long MD simulations,[38] with only small conformational changes, fully within the thermal fluctuations, at the ApT step of the minor groove. The major determinant for the DNA structure stability was attributed to electrostatic effects arising from the hydration electrostatics, the counterion atmosphere, the phosphate repulsions, and the groove-bound counterions. Several other studies have also addressed ion and solvent influences on DNA structure. A narrowing of the minor groove of DNA of the EcoRI

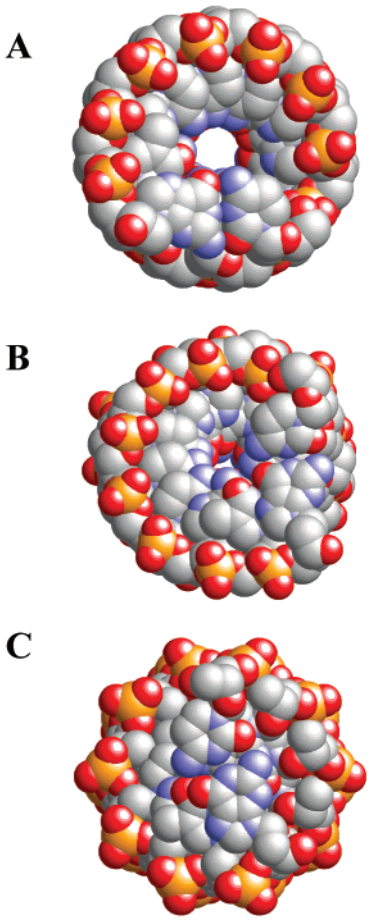

FIGURE 2. View down the helix axis of the DNA dodecamer d(CATCCCGGGATG)$_2$ in (A) canonical A conformation, (B) conformation intermediate between A and B, PDB ID 1DC0,[35] and (C) canonical B conformation.

dodecamer[39] was found when cations interact with the DNA bases in the minor groove to generate an internal ion-spine of hydration and also when the ions interact with the phosphate groups in the ApT sequence and the water molecules, directly with the DNA bases. In MD simulations of the EcoRI dodecamer, three other DNA duplexes, and one RNA duplex, in part to evaluate the newly developed nucleic acid force field parameters[13] of CHARMM, the B form of the DNA oligonucleotides was maintained throughout the simulations in aqueous solution, whereas in 75% ethanol, the A form of DNA was stabilized.[40] Differences in hydrogen bonding to the solvent were also observed in simulations[41] of the DNA duplex d(CGCGCG)$_2$ at different temperatures ranging from 20 to 340 K. The temperature dependence of the amplitude of the mean square fluctuations of the DNA atoms was linear below the glass temperature at ~230 K, which is consistent with experiment. At this temperature, a maximum number of hydrogen bonds between the duplex and the water molecules was found, whereas a decrease in average lifetime of hydrogen bonds to water was observed for increasing temperature. In a simulation of d(TATGGATCCATA)$_2$, which is recognized by the BamHI endonuclease, a transformation from the initial canonical B-DNA form to the B-like form in the X-ray structure was observed,[42] and the guanine−cytosine base pairs were more hydrated than the adenine−thymine base pairs in both the major and minor groove, and the residence times of the water molecules were longer in the minor groove, as compared to the major groove.

DNA bending has been observed in simulations of two A-tract DNA dodecamers.[43] The results agreed with both the junction model, in which the bend on the 5′ side of the A tract was seen as a positive roll of 12°, and the wedge model, in which the bend occurred gradually at each base pair step of the A tract. The bend in the A tract was stabilized by the propeller twisting of adenine−thymine base pairs, differences in the deoxyribose puckering of adenine and thymine, a narrow minor groove, and a preserved hydration spine. A set of 14-base-pair B-DNA duplexes containing the TATA element, which is bent when complexed with TATA-box binding protein (TBP), have been investigated,[44] and several parameters, including overall flexibility, widening of the minor groove at the ends of the TATA element, untwisting within the TATA element together with a large roll at the ends, and relatively low maximal water densities surrounding the DNA, were pointed out to be essential for TBP activity.

Imperfections in the base pairing can be tolerated with only minor disturbances to the surrounding DNA duplex, as shown in simulations of a DNA octamer containing an adenine bulge.[45] The simulations suggested a pathway for the transition between the stacked and looped-out conformations, which were in very good agreement with NMR and X-ray structures. The zipper-like duplex d(GCGAAAGC)$_2$ has a central core of four unpaired adenines that are flanked by sheared guanine−adenine base pairs, and in a simulation study, the conformation of the zipper base pairs was maintained by penetration of monovalent ions into the hydration shell.[46] Stacking of neighboring bases was important for keeping the guanine−adenine mismatch base pairs intact, and replacing a zipper adenine with a cytosine, guanine, or thymine yielded stable zipper conformations when purines were incorporated into the zipper, whereas the pyrimidines showed much more unstable structures.

Dynamical properties of DNA, relaxation times, order parameters, and effective correlation times, were determined from MD trajectories of two DNA duplexes,[47] d(TCGCG)$_2$ and d(CGCGCG)$_2$ and compared to NMR relaxation measurements. For the nonterminal nucleotides, the T_1 relaxation times were in reasonable agreement with experiment. The order parameters were quite well reproduced, whereas the effective correlation times were clearly smaller than the experimental estimates. Later, these effective correlation times were confirmed in MD simulations and ^{13}C NMR relaxation measurements of (CGCAAATTTGCG)$_2$ in which the calculated order parameters were ~0.82 and the effective correlation times ~13 ps, which is in good agreement with experimental data.[48]

Recent advances in nanomanipulation methods have sparked an interest also in theoretical studies of the deformation of DNA molecules as a result of a forced

Table 1. Pair-Wise RMSD (Å) between the Dodecamer 1DC0[35] and the Same Sequence in Canonical A and B Forms, and between the Dickerson Dodecamer 1BNA[36] and Its Sequence in A and B Forms

structures	all[a]	bases[b]	backbone[c]	all 4−9[d]	bases 4−9	backbone 4−9	Pyr[e] 4−9	Pur[f] 4−9
ADNA vs BDNA	6.56	5.60	7.28	3.01	2.00	3.66	1.88	1.95
ADNA vs 1DC0	3.34	2.95	3.63	1.45	0.87	1.80	0.84	0.82
BDNA vs 1DC0	4.39	3.64	4.96	2.27	1.38	2.81	1.21	1.44
ADNA vs 1BNA	6.31	5.50	6.90	2.92	1.82	3.58	1.25	0.87
BDNA vs 1BNA	1.31	0.94	1.55	0.84	0.44	1.04	0.29	0.35

[a] All non-hydrogen atoms. [b] All non-hydrogen base atoms. [c] All non-hydrogen sugar−phosphate atoms. [d] The non-hydrogen atoms of the six middle base pairs. [e] The pyrimidine non-hydrogen base atoms. [f] The purine non-hydrogen base atoms.

extension. MD simulations in vacuo were used to model the extended conformations due to the increasing magnitude of the forces that were applied to the opposing 3′ ends of DNA dodecamer strands.[49] The DNA strands separated directly when the forces were from 0.80 to 1.45 nN, which is similar in magnitude to the experimentally measured force. For forces between 0.065 and 0.090 nN, an extension was seen, and this generated a ladder structure with bases from one strand stacked on the bases of the other. Potential of mean force calculations based on MD simulations in solution have been performed to analyze the elasticity[50] of a DNA dodecamer, which was extended without any barrier from a length shorter than A-DNA to a length longer than 2.4 times the B-DNA contour length. At this point, the strand−strand separation barrier was reached, and the favorable dodecamer−solvent interactions could no longer compensate for the interstrand repulsion. At the separation, the calculated force was 0.09 nN, close to the 0.13 nN estimated from direct AFM measurements.

Molecular dynamics simulations let us follow in great detail processes such as the A-to-B-DNA transition or the stretching of DNA, and also allow us to begin to provide reliable data on the importance of the hydration and ionic atmosphere of DNA.

RNA

The range of structures and activities to investigate is greater for RNA than for DNA, and after describing some comparative studies of DNA and RNA helices, we shift the focus to structures that are more characteristic of RNA systems.

Several MD simulations have shown that double-stranded RNA oligomers are stable A-RNA conformations in aqueous solution. The RNA dodecamer duplex $r(GC)_6$ was very stable at both normal pressure and 6000 atm,[51] with smaller fluctuations at the higher pressure. In a study of the RNA dodecamer $r(GGACUUCGGUCC)_2$, the focus was on the water-mediated uracil−cytosine base pairs.[52] From the MD simulation, one conformation, which was in close agreement with the water-mediated uracil−cytosine pair in the X-ray structure, was observed. Here, water has two tasks as hydrogen bonding acceptor and donor. A second conformation was also found in which the water molecule was connected to two donor sites. During a short event in the MD simulation, a direct uracil−cytosine base-pair structure was seen. These water-mediated conformations involving water molecules with very long residence times provide an example of stabilizing interactions, which are difficult to study experimentally. Hydration, together with dynamics and counterion behavior, has also been studied for the A-RNA $r(CG)_{12}$ and $r(UA)_{12}$, as well as for the B-DNA $d(CG)_{12}$ and $d(TA)_{12}$ duplexes.[53,54] The study clearly found a higher flexibility for the DNA helix, as compared to the RNA helix, as has previously been seen.[51] The RNA duplexes had more-well-defined hydration patterns than the DNA structures, with the d(A−T) base pairs being less hydrated, with about 1−2 water molecules, than the r(G═C), r(A−U), and d(G═C) base pairs. In the first hydration shell, the residence times of water molecules were ∼0.5−1 ns, with nonsequence-dependent hydration patterns in RNA, whereas in DNA, long-lived sequence-dependent hydration patterns were observed, essentially in the minor groove. Further, the potassium counterions were mainly bound to major groove atoms of d(GC), r(GC), and r(AU). The number of ions in the first hydration shell was 0.5/base pair for all duplexes. In the G,C duplexes, the K^+ ions bound mainly to the GC steps and not to CG.

The hairpin, a helical stem capped by a loop at one end, is the most common structural feature in RNA. Hairpin II of U1 small nuclear RNA, with 5 base pairs in the stem and 10 bases in the loop, was simulated both in complex with the U1A protein and free in solution.[16] The loop in the free hairpin was very flexible, but the loop and also the stem of the RNA became more ordered upon binding to the protein. Several simulations have been performed of hairpins with small, very stable tetraloops. For GNRA tetraloops (where N is any base and R is a purine), a stabilizing water molecule in the loop with residence time approaching that of the simulation has been reported.[55,56] The hairpin simulated by Sarzynska et al,[56] the D loop of 5S rRNA, also contained an extra, unpaired U in the stem part, and simulations were performed with this U either flipped out into the solvent or as part of the helical stack. Both setups gave reasonable and stable structures, and on the basis of comparison with experimental patterns of susceptibility to lead induced phosphoester cleavage, it was suggested that both conformations would be populated in solution. The UUCG loop sequence, which belongs to the UNCG tetraloop family, has been simulated as part of an RNA aptamer[52] as well as in a hairpin,[57−60] where conversion from an incorrect to a correct structure was facilitated by changing the sugars in the loop to deoxyriboses[57] or by using a locally enhanced sampling method.[59] The UUCG tetraloop stability has been further characterized by free-energy perturbation calculations showing the sequence depen-

dence of the stabilizing effect of the 2'-OH group[60] and by free-energy evaluations of snapshots from an MD trajectory using a continuum model.[58]

The first RNA for which a simulation was undertaken was a tRNA,[4] and since then, the tRNA structure, in particular the anticodon hairpin, has been the subject of several simulation studies. Hydration analysis of the $tRNA^{Asp}$ anticodon hairpin[61] showed that the phosphate oxygens had the largest accessibility to water. Water bridges between the phosphate oxygens with long residence times were found to stabilize the RNA backbone. For the 2′-hydroxyl groups, tertiary contacts as well as hydration were observed. Therefore, these groups were suggested not to be involved in stabilizing the helical regions of the RNA molecules. Specific hydration was also observed for some bases, with two different hydration patterns identified for the G−U base pairs. Pseudouridine and 1-methylguanine-37 were also stabilized by water molecules with long residence times. These water molecules, close to specific RNA atoms, were associated cooperatively with other RNA atoms. Two strongly favored binding sites were predicted for NH_4^+ ions in the anticodon loop. In another study[62] of the complexes between the anticodon of yeast $tRNA^{Phe}$ with cognate (UUC) and noncognate codon (UUU) trinucleotides, small conformational differences for the free and bound complexes were observed close to the Y37 base. This base displayed larger root-mean-square fluctuations when the UUC codon was present. An enhanced stability in the loop was seen when the codon was bound. The other arm of the tRNA, the amino acid acceptor arm, has also been studied in simulations[63,64] of RNA minihelices that mimic the acceptor stem of $tRNA^{Ala}$, which has all the determinants for recognition by the synthetase contained in this stem. These minihelices are hairpins closed by a tetraloop and with a dangling $A_{73}C_{74}C_{75}A_{76}$-3′ end. The simulations showed a positive correlation of the aminoacylation activity with the tendency of the base at position 73 to stack on G_1.[64] It was furthermore observed that the wild-type G_3/U_{70} wobble base pair in the middle of the stem, in contrast to other base pairs at this position, strongly binds a water molecule in the minor groove,[63] and the strength of this water binding also correlates with aminoacylation activity. A simulation of the complete yeast $tRNA^{Asp}$ molecule including 74 NH_4^+ counterions and explicit water molecules showed that secondary and tertiary contacts were well-preserved[65] although the base triples in the core of the tRNA were slightly more labile. This was suggested to be due to the "weak" hydrogen-bonding pattern of the base triples and the different ionic environment, in particular, the absence of Mg^{2+} ions, in the simulated system.

MD simulations of the hammerhead ribozyme RNA preserved the overall structure with well-maintained base pairs and tertiary interactions, except for the 2′-OH groups, which were more flexible.[66] In the crystal structure of this ribozyme, the region around the scissile bond is not in a catalytically competent conformation.[66,67] The main findings of the simulations were an in-plane breathing motion for the adenine in the two sheared guanine·adenine base pairs and from a constrained simulation an activating conformational change at the cleavage-site cytosine-17, which might be affected by the structural changes in the sugar puckering of the turn residues. A two-metal ion mechanism with a microbridging OH^- ion positioned between two Mg^{2+} ions was suggested for hammerhead ribozyme catalysis.[68] The activation of the catalysis occurred from the deep groove side of stem I where the 2′-hydroxyl nucleophile attacks the cleavable phosphate. A minor local change of a ribose from a C3′-endo to a C2′-endo conformation was observed. This small structural difference was suggested to be enough to initiate the cleavage reaction. In another study,[69] the torsion angles of the phosphate linkage of cytosine-17 were rotated from the cleavage site toward the solvent, and during the simulation, near-attack conformations were formed, with one Mg^{2+} ion coordinated close to the 2′-hydroxyl oxygen. The results of this study, thus, are consistent with a one-metal ion mechanism of catalysis. These are two carefully performed simulation studies, but the two Mg^{2+} ions that are used in the two-metal mechanism have only 50% occupancy in the PDB file, which may indicate that they represent alternative sites, not two simultaneously present ions.

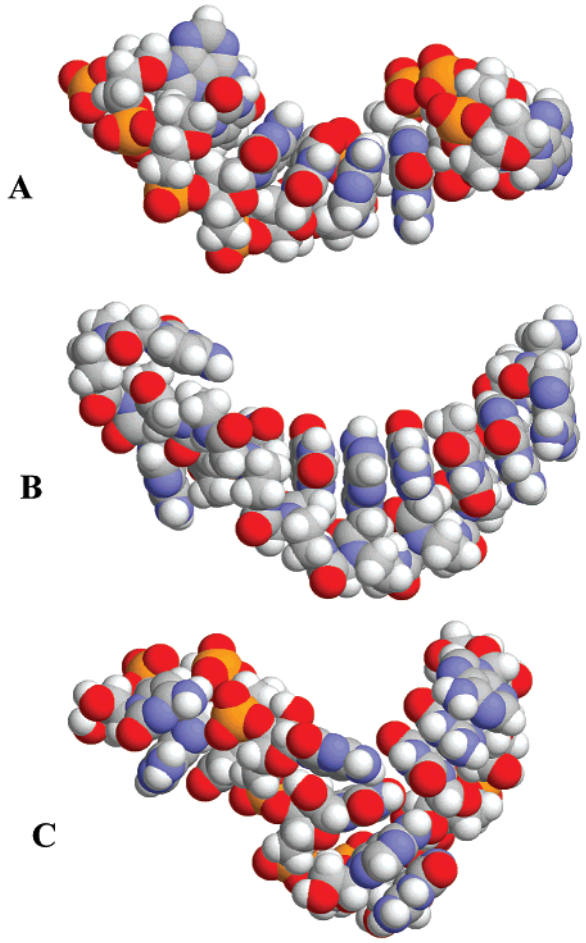

FIGURE 3. Snapshots from MD simulations of single-stranded (A) DNA, (B) PNA, and (C) RNA oligonucleotides.

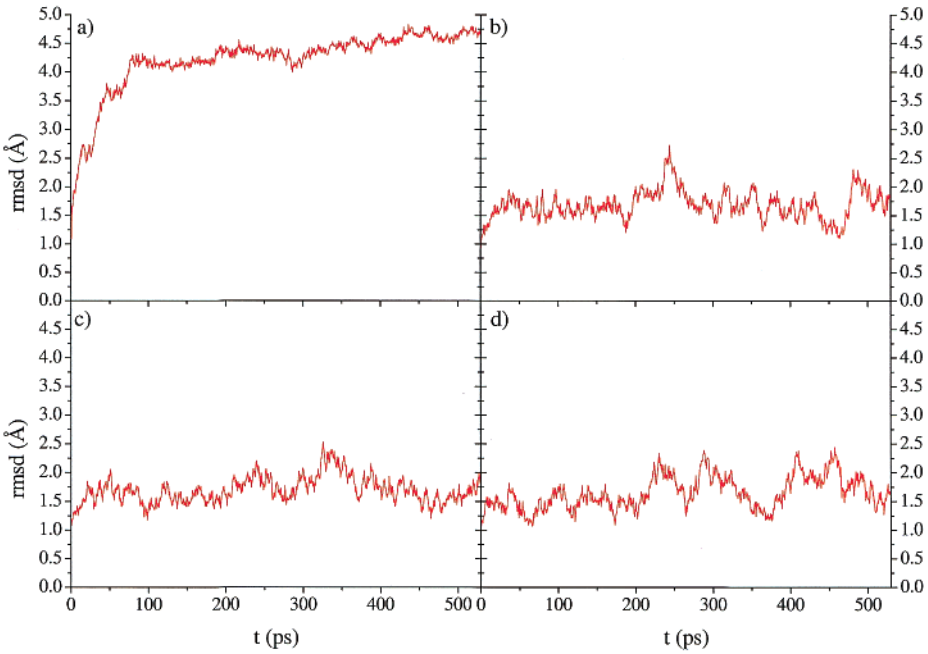

FIGURE 4. RMSD from the initial conformation vs time from MD simulations[77] of the DNA duplex d(CGCGCG)$_2$ using (a) group-based switching truncation at 12.0 Å and periodic boundary conditions, (b) particle mesh Ewal summation and periodic boundary conditions, (c) atom-based force-shifting truncation at 12.0 Å and periodic boundary conditions, and (d) atom-based force-shifting at 12.0 Å and stochastic boundary conditions.

PNA

PNA molecules are nucleic acid homomorphs with regular nitrogen bases attached to an uncharged peptide backbone. Because they may form both double- and triple-stranded structures with regular nucleic acids with high affinity, PNA molecules are very interesting as drug candidates. A few MD simulation studies of PNA molecules have been carried out, either as single strands or in various combinations with other PNA, DNA, or RNA strands. A recent MD study analyzed single-stranded DNA, PNA, and RNA with the same base sequence.[70] The initial base-stacked conformation in the PNA strand was maintained in the whole MD simulation, whereas unstacking events were observed for the DNA and RNA strands (Figure 3). Further findings included a decreased correlation between the backbone and bases in the PNA strand due to the weaker physical coupling compared to the DNA and RNA forms. The largest flexibility was seen for the RNA strand and the stiffest was the PNA strand. Backbone−water interactions were weaker for the PNA strand as a result of the more hydrophobic character of its backbone.

Studies of PNA-containing duplexes have shown more B-DNA-like properties for the parallel PNA−DNA duplex, whereas the PNA−PNA and antiparallel PNA−DNA duplexes showed structures in both the A and B forms.[71] The base linker region also displayed restricted flexibility in the PNA strands. PNA−DNA and PNA−RNA duplexes with three different starting structures in A-like, B-like, and $P_{A/B}$-like forms have also been studied using MD simulations,[72] and here, too, the three MD trajectories of the PNA−DNA duplex converged toward the P_B form. For the PNA−RNA duplex, a P_A form was obtained for the MD simulations started from the A and P_A forms. The PNA−RNA MD simulation, which was started from the P_B form, unfolded in the first 500 ps. PNA was found to have a more flexible backbone than DNA or RNA, but this does not affect the stacking arrangement of the bases.

A PNA−DNA−PNA triple helix was investigated using three different structures as starting conformations for the MD simulations,[73] which all converged to a structure ensemble close to the crystal structure. Further, it was observed that the hydrogen bonds among the amide hydrogens of the PNA strand and the phosphate oxygens of the DNA strand were changed, and instead, water-mediated hydrogen bonds occurred. This was suggested not to have affected the stability of the triplex, but to have changed the groove widths. When compared to a DNA−DNA−DNA triplex, the PNA−DNA−PNA triplex has different helical features but similar base stacking interactions, and therefore, the driving force is due to specific conformational preferences of the PNA strands.

Long-Range Electrostatic Effects

Electrostatic effects are very important for the stability of highly charged nucleic acids,[74] and recently, the particle mesh Ewald method has become very popular in MD simulation studies.[75] A large number of nucleic acid systems have been investigated using this method and have been found to produce accurate and stable trajectories,[9,10] but other techniques have been developed for the truncation of long-range interactions.[76] A number of truncation methods have recently been evaluated by MD simulations of a DNA hexamer in aqueous solution.[77] The atom-based force-shift truncation method, using a 12-Å cutoff, and the particle mesh Ewald (PME) method

produced stable and very similar nanosecond MD simulations of the DNA molecule, whereas some truncation methods using charge groups or a switching function applied to the electrostatic energy over an interval before the cutoff resulted in either completely collapsed or hyperstable DNA structures (Figure 4). The choice, thus, seems to be not between Ewald summation methods and spherical truncation, but rather between one of the well-behaved methods (including Ewald summation, and several spherical truncation schemes) and the pathological truncation schemes—perhaps not a very surprising conclusion, but nevertheless a useful result, since it shows that also nonperiodic systems may be appropriately handled. The pros and cons of the Ewald summation method and the periodicity it imposes on the system have been the subject of a number of studies indicating that the artifacts are small for biomolecular systems.[78] With optimized cutoff radius and convergence parameters for the PME summation, the CPU time requirements are similar, but the periodic boundary conditions necessary with standard implementations of PME makes it slower than a spherical cutoff in a nonperiodic geometry adapted to the shape of the system being studied.

Conclusion and Future Perspectives

Current energy functions and simulation protocols allow stable and apparently realistic simulations of nucleic acids over several nanoseconds, and we can obtain relevant information about the influence of the nucleotide sequence and various solvent conditions on the structure and dynamics of molecules as large as tRNA. Two key aspects resulting from the very detailed information obtained in simulations, giving an advantage over experimental studies, is that processes such as conformational transitions may be monitored at a very detailed level, and the ability to follow closely the behavior of solvent molecules and their interactions with the solute. It is reasonable to expect that soon it will be possible to approach problems involving large biomolecular complexes with nucleic acids, as well as on a time scale of hundreds of nanoseconds, but more complicated reactions, such as RNA catalysis and folding, are also likely to be tackled, even though they may require even more computing power.

References

(1) McCammon, J. A.; Gelin, B. R.; Karplus, M. Dynamics of Folded Proteins. *Nature* **1977**, *267*, 585−590.
(2) Levitt, M. Computer Simulation of DNA Double Helix Dynamics. *Cold Spring Harbor Symp. Quantum Biol.* **1983**, *47*, 251−261.
(3) Tidor, B.; Irikura, K. K.; Brooks, B. R.; Karplus, M. Dynamics of DNA Oligomers. *J. Biomol. Struct. Dyn.* **1983**, *1*, 231−252.
(4) Prabhakaran, M.; Harvey, S. C.; Mao, B.; McCammon, J. A. Molecular dynamics of phenylalanine transfer RNA. *J. Biomol. Struct. Dyn.* **1983**, *1*, 357−369.
(5) Nordlund, T. M.; Andersson, S.; Nilsson, L.; Rigler, R.; Graeslund, A.; McLaughlin, L. W. Structure and Dynamics of a Fluorescent DNA Oligomer Containing the Ecori Recognition Sequence: Fluorescence, Molecular Dynamics, and NMR Studies. *Biochemistry* **1989**, *28*, 9095−1003.
(6) Nilsson, L.; Karplus, M. Molecular Dynamics Simulation of the Anticodon Arm of Phenylalanine Transfer RNA. *NATO Asi Ser. Ser. C.* **1986**, *110*, 151−159.
(7) Seibel, G. L.; Singh, U. C.; Kollman, P. A. A molecular dynamics simulation of double helical B-DNA including counterions and water. *Proc. Natl. Acad. Sci. U.S.A.* **1985**, *82*, 6537−6540.
(8) Auffinger, P.; Westhof, E. Simulations of the Molecular Dynamics of Nucleic Acids. *Curr. Op. Struct. Biol.* **1998**, *8*, 227−236.
(9) Beveridge, D. L.; McConnell, K. J. Nucleic acids: theory and computer simulation, Y2K. *Curr. Opin. Struct. Biol.* **2000**, *10*, 182−196.
(10) Cheatham III, T. E.; Kollman, P. A. Molecular Dynamics Simulation Of Nucleic Acids. *Annu. Rev. Phys. Chem.* **2000**, *51*, 435−471.
(11) MacKerell Jr, A. D.; Nilsson, L. In *Computational Biochemistry and Biophysics*; Becker, O., MacKerell, A. D., Jr., Roux, B., Watanabe, M., Eds.; Marcel Dekker: New York, 2001; pp 441−464.
(12) Cornell, W. D.; Cieplak, P.; Bayly, C. I.; Gould, I. R.; Merz, K. M.; Ferguson, D. M.; Spellmeyer, D. C.; Fox, T.; Caldwell, J. W.; Kollman, P. A. A Second Generation Force Field for the Simulation of Proteins, Nucleic Acids, and Organic Molecules. *J. Am. Chem. Soc.* **1995**, *117*, 5179−5197.
(13) Foloppe, N.; MacKerell, A. D., Jr. All-Atom Empirical Force Field for Nucleic Acids: I. Parameter Optimization Based on Small Molecule and Condensed Phase Macromolecular Target Data. *J. Comput. Chem.* **2000**, *21*, 86−104.
(14) Eriksson, M. A. L.; Nilsson, L. Structure, Thermodynamics and Cooperativity of the Glucocorticoid Receptor DNA-Binding Domain in Complex With Different Response Elements—Molecular Dynamics Simulation and Free Energy Perturbation Studies. *J. Molec. Biol.* **1995**, *253*, 453−472.
(15) Tang, Y.; Nilsson, L. Interaction of human SRY protein with DNA: A molecular dynamics study. *Proteins: Struct. Funct. Genet.* **1998**, *31*, 417−433.
(16) Tang, Y.; Nilsson, L. Molecular dynamics simulations of the complex between human U1A protein and hairpin II of U1 small nuclear RNA and of free RNA in solution. *Biophys. J.* **1999**, *77*, 1284−305.
(17) Tang, Y.; Nilsson, L. Effect of G40R mutation on the binding of human SRY protein to DNA: A molecular dynamics view. *Proteins: Struct. Funct. Genet.* **1999**, *35*, 101−113.
(18) Tomic, S.; Nilsson, L.; Wade, R. C. Nuclear receptor−DNA binding specificity: A COMBINE and Free- Wilson QSAR analysis. *J. Med. Chem.* **2000**, *43*, 1780−1792.
(19) Sen, S.; Nilsson, L. Structure, interaction, dynamics and solvent effects on the DNA−EcoRI complex in aqueous solution from molecular dynamics simulation. *Biophys. J.* **1999**, *77*, 1782−800.
(20) Sen, S.; Nilsson, L. Free energy calculations and molecular dynamics simulations of wild-type and variants of the DNA−EcoRI complex. *Biophys. J.* **1999**, *77*, 1801−10.
(21) Eriksson, M. A.; Nilsson, L. Structural and dynamic differences of the estrogen receptor DNA-binding domain, binding as a dimer and as a monomer to DNA: molecular dynamics simulation studies [published erratum appears in *Eur. Biophys. J.* **1999**, *28* (4), 356]. *Eur. Biophys. J.* **1999**, *28*, 102−111.
(22) Eriksson, M. A.; Nilsson, L. Structural and dynamic effects of point mutations in the recognition helix of the glucocorticoid receptor DNA-binding domain. *Protein Eng.* **1998**, *11*, 589−600.
(23) Norberg, J.; Nilsson, L. Stacking−Unstacking of the Dinucleoside Monophosphate Guanylyl-3′,5′-Uridine Studied With Molecular Dynamics. *Biophys. J.* **1994**, *67*, 812−824.
(24) Norberg, J.; Nilsson, L. High-Pressure Molecular Dynamics of a Nucleic Acid Fragment. *Chem. Phys. Lett.* **1994**, *224*, 219−224.
(25) Barciszewski, J.; Jurczak, J.; Porowski, S.; Specht, T.; Erdmann, V. A. The Role of Water structure in conformational changes of nucleic acids in ambient and high-pressure conditions. *Eur. J. Biochem.* **1999**, *260*, 293−307.
(26) Lee, H.; Darden, T.; Pedersen, L. Accurate crystal molecular dynamics simulations using particle-mesh-Ewald: RNA dinucleotides—ApU and GpC. *Chem. Phys. Lett.* **1995**, *243*, 229−235.
(27) Norberg, J.; Nilsson, L. Stacking Free Energy Profiles For All 16 Natural Ribodinucleoside Monophosphates in Aqueous Solution. *J. Am. Chem. Soc.* **1995**, *117*, 10832−10840.
(28) Norberg, J.; Nilsson, L. Potential of Mean Force Calculations of the Stacking Unstacking Process in Single-Stranded Deoxyribodinucleoside Monophosphates. *Biophys. J.* **1995**, *69*, 2277−2285.
(29) Norberg, J.; Nilsson, L. Temperature Dependence of the Stacking Propensity of Adenylyl-3′,5′-Adenosine. *J. Phys. Chem.* **1995**, *99*, 13056−13058.
(30) Mohan, V.; Griffey, R. H.; Davis, D. R. Structure and Dynamics of MMI Linked Nucleotides. *Tetrahedron* **1995**, *51*, 6855−6868.
(31) Giraldo, J.; Wodak, S. J.; van Belle, D. Conformational Analysis of GpA and GpAp in Aqueous Solution by Molecular Dynamics and Statistical Methods. *J. Mol. Biol.* **1998**, *283*, 863−882.
(32) Norberg, J.; Nilsson, L. Conformational Free Energy Landscape of ApApA from Molecular Dynamics Simulations. *J. Phys. Chem. A.* **1996**, *100*, 2550−2554.

(33) Norberg, J.; Nilsson, L. Influence of adjacent bases on the stacking−unstacking process of single-stranded oligonucleotides. *Biopolymers* **1996**, *39*, 765−768.
(34) Norberg, J.; Nilsson, L. Solvent Influence on Base Stacking. *Biophys. J.* **1998**, *74*, 394−402.
(35) Ng, H.-L.; Kopka, M. L.; Dickerson, R. E. The structure of a stable intermediate in the A ↔ B DNA helix transition. *Proc. Natl. Acad. Sci. U.S.A.* **2000**, *97*, 2035−2039.
(36) Drew, H. R.; Dickerson, R. E. Structure of a B-DNA Dodecamer. III. Geometry of Hydration. *J. Mol. Biol.* **1981**, *151*, 535−556.
(37) Foloppe, N.; MacKerell Jr, A. D. Intrinsic Conformational Properties of Deoxyribonucleosides: Implicated Role for Cytosine in the Equilibrium Among the A, B, and Z Forms of DNA. *Biophys. J.* **1999**, *76*, 3206−3218.
(38) McConnell, K. J.; Beveridge, D. L. DNA Structure: What's in Charge? *J. Mol. Biol.* **2000**, *304*, 803−820.
(39) Hamelberg, D.; McFail-Isom, L.; Williams, L. D.; Wilson, W. D. Flexible Structure of DNA: Ion Dependence of Minor-Groove Structure and Dynamics. *J. Am. Chem. Soc.* **2000**, *122*, 10513−10520.
(40) MacKerell, A. D., Jr.; Banavali, N. K. All-Atom Empirical Force Field for Nucleic Acids: II. Application to Molecular Dynamics Simulations of DNA and RNA in Solution. *J. Comput. Chem.* **2000**, *21*, 105−120.
(41) Norberg, J.; Nilsson, L. Glass transition in DNA from molecular dynamics simulations. *Proc. Natl. Acad. Sci.* **1996**, *93*, 10173−10176.
(42) Castrignano, T.; Chillemi, G.; Desideri, A. Structure and Hydration of BamHI DNA Recognition Site: A Molecular Dynamics Investigation. *Biophys. J.* **2000**, *79*, 1263−1272.
(43) Strahs, D.; Schlick, T. A-tract Bending: Insight into Experimental Structures by Computational Models. *J. Mol. Biol.* **2000**, *301*, 643−663.
(44) Qian, X.; Strahs, D.; Schlick, T. Dynamic Simulations of 13 TATA Variants Refine Kinetic Hypotheses of Sequence/Activity Relationships. *J. Mol. Biol.* **2001**, *308*, 681−703.
(45) Feig, M.; Zacharias, M.; Pettitt, B. M. Conformations of an Adenine Bulge in a DNA Octamer and Its Influence on DNA Structure from Molecular Dynamics Simulations. *Biophys. J.* **2001**, *81*, 352−370.
(46) Spacková, N.; Berger, I.; Sponer, J. Nanosecond Molecular Dynamics of Zipper-like DNA Duplex Structures Containing Sheared G−A Mismatch Pairs. *J. Am. Chem. Soc.* **2000**, *122*, 7564−7572.
(47) Norberg, J.; Nilsson, L. Internal Mobility of the Oligonucleotide Duplexes $d(TCGCG)_2$ and $d(CGCGCG)_2$ in Aqueous Solution From Molecular Dynamics Simulations. *J. Biomol. NMR* **1996**, *7*, 305−314.
(48) Gaudin, F.; Genest, D.; Lancelot, G. Internal dynamics of $d(CGCAAATTTGCG)_2$: a comparison of NMR relaxation measurements with a molecular dynamics simulation. *Eur. Biophys. J.* **1997**, *26*, 239−245.
(49) Konrad, M. W.; Bolonick, J. I. Molecular Dynamics Simulation of DNA Stretching Is Consistent with the Tension Observed for Extension and Strand Separation and Predicts a Novel Ladder Structure. *J. Am. Chem. Soc.* **1996**, *118*, 10989−10994.
(50) MacKerell, A. D., Jr.; Lee, G. U. Structure, force, and energy of a double-stranded DNA oligonucleotide under tensile loads. *Eur. Biophys. J.* **1999**, *28*, 415−426.
(51) Norberg, J.; Nilsson, L. Constant Pressure Molecular Dynamics Simulations of the Dodecamers $d(GCGCGCGCGCGC)_2$ and $r(GCGCGCGCGCGC)_2$. *J. Chem. Phys.* **1996**, *104*, 6052−6057.
(52) Schneider, C.; Brandl, M.; Sühnel, J. Molecular Dynamics Simulation Reveals Conformational Switching of Water Mediated Uracil−Cytosine Base-pairs in an RNA Duplex. *J. Mol. Biol.* **2001**, *305*, 659−667.
(53) Auffinger, P.; Westhof, E. Water and Ion Binding Around RNA and DNA (C, G) Oligomers. *J. Mol. Biol.* **2000**, *300*, 1113−1131.
(54) Auffinger, P.; Westhof, E. Water and Ion Binding Around $r(UpA)_{12}$ and $d(TpA)_{12}$ Oligomers−Comparison with RNA and DNA $(CpG)_{12}$ Duplexes. *J. Mol. Biol.* **2001**, *305*, 1057−1072.
(55) Zichi, D. A. Molecular Dynamics of RNA with the OPLS Force Field. Aqueous Simulation of a Hairpin Containing a Tetranucleotide Loop. *J. Am. Chem. Soc.* **1995**, *117*, 2957−2969.
(56) Sarzynska, J.; Kulinski, T.; Nilsson, L. Conformational Dynamics of a 5S rRNA Hairpin Domain Containing Loop D and a Single Nucleotide Bulge. *Biophys. J.* **2000**, *79*, 1213−1227.
(57) Miller, J. L.; Kollman, P. A. Theoretical Studies of an Exceptionally Stable RNA Tetraloop: Observation of Convergence from an Incorrect NMR Structure to the Correct One Using Unrestrained Molecular Dynamics. *J. Mol. Biol.* **1997**, *270*, 436−450.
(58) Srinivasan, J.; Miller, J.; Kollman, P. A.; Case, D. A. Continuum Solvent Studies of the Stability of RNA Hairpin Loops and Helices. *J. Biomol. Struct. Dyn.* **1998**, *16*, 671−682.
(59) Simmerling, C.; Miller, J. L.; Kollman, P. A. Combined Locally Enhanced Sampling and Particle Mesh Ewald as a Strategy To Locate the Experimental Structure of a Nonhelical Nucleic Acid. *J. Am. Chem. Soc.* **1998**, *120*, 7149−7155.
(60) Williams, D. J.; Hall, K. B. Experimental and Theoretical Studies of the Effects of Deoxyribose Substitutions on the Stability of the UUCG Tetraloop. *J. Mol. Biol.* **2000**, *297*, 251−265.
(61) Auffinger, P.; Westhof, E. RNA Hydration: Three Nanoseconds of Multiple Molecular Dynamics Simulations of the Solvated $tRNA^{Asp}$ Anticodon Hairpin. *J. Mol. Biol.* **1997**, *269*, 326−341.
(62) Lahiri, A.; Nilsson, L. Molecular Dynamics of the Anticodon Domain of Yeast $tRNA^{Phe}$: Codon−anticodon Interaction. *Biophys. J.* **2000**, *79*, 2276−2289.
(63) Nagan, M. C.; Kerimo, S. S.; Musier-Forsyth, K.; Cramer, C. J. Wild-Type RNA Microhelix Ala and 3:70 Variants: Molecular Dynamics Analysis of Local Helical Structure and Tightly Bound Water. *J. Am. Chem. Soc.* **1999**, *121*, 7310−7317.
(64) Nagan, M. C.; Beuning, P.; Musier-Forsyth, K.; Cramer, C. J. Importance of discriminator base stacking interactions: molecular dynamics analysis of A73 microhelix^{Ala} variants. *Nucleic Acids Res.* **2000**, *28*, 2527−2534.
(65) Auffinger, P.; Louise-May, S.; Westhof, E. Molecular Dynamics Simulations of Solvated Yeast $tRNA^{Asp}$. *Biophys. J.* **1999**, *76*, 50−64.
(66) Hermann, T.; Auffinger, P.; Westhof, E. Molecular dynamics investigations of hammerhead ribozyme RNA. *Eur. Biophys. J.* **1998**, *27*, 153−165.
(67) Scott, W. G.; Murray, J. B.; Arnold, J. R. P.; Stoddard, B. L.; Klug, A. Capturing the Structure of a Catalytic RNA Intermediate: The Hammerhead Ribozyme. *Science* **1996**, *274*, 2065−2069.
(68) Hermann, T.; Auffinger, P.; Scott, W. G.; Westhof, E. Evidence for a hydroxide ion bridging two magnesium ions at the active site of the hammerhead ribozyme. *Nucleic Acids Res.* **1997**, *25*, 3421−3427.
(69) Torres, R. A.; Bruice, T. C. Molecular dynamics study displays near in-line attack conformations in the hammerhead ribozyme self-cleavage reaction. *Proc. Natl. Acad. Sci. U.S.A.* **1998**, *95*, 11077−11082.
(70) Sen, S.; Nilsson, L. MD Simulations of Homomorphous PNA, DNA, and RNA Single Strands: Characterization and Comparison of Conformations and Dynamics. *J. Am. Chem. Soc.* **2001**, *123*, 7414−7422.
(71) Sen, S.; Nilsson, L. Molecular dynamics of duplex systems involving PNA: Structural and dynamical consequences of the nucleic acid backbone. *J. Am. Chem. Soc.* **1998**, *120*, 619−631.
(72) Soliva, R.; Sherer, E.; Luque, F. J.; Laughton, C. A.; Orozco, M. Molecular Dynamics Simulations of PNA−DNA and PNA−RNA Duplexes in Aqueous Solution. *J. Am. Chem. Soc.* **2000**, *122*, 5997−6008.
(73) Shields, G. C.; Laughton, C. A.; Orozco, M. Molecular Dynamics Simulation of a PNA−DNA−PNA Triple Helix in Aqueous Solution. *J. Am. Chem. Soc.* **1998**, *120*, 5895−5904.
(74) Harvey, S. C. Treatment of Electrostatic Effects in Macromolecular Modeling. *PROTEINS* **1989**, *5*, 78−92.
(75) Sagui, C.; Darden, T. A. Molecular Dynamics Simulations of Biomolecules: Long-Range Electrostatic Effects. *Annu. Rev. Biophys. Biomol. Struct.* **1999**, *28*, 155−179.
(76) Steinbach, P. J.; Brooks, B. R. New Spherical-Cutoff Methods For Long-Range Forces in Macromolecular Simulation. *J. Comput. Chem.* **1994**, *15*, 667−683.
(77) Norberg, J.; Nilsson, L. On the Truncation of Long-Range Electrostatic Interactions in DNA. *Biophys. J.* **2000**, *79*, 1537−1553.
(78) Hünenberger, P. H.; McCammon, J. A. Ewald artifacts in computer simulations of ionic solvation and ion−ion interaction: A continuum electrostatics study. *J. Chem. Phys.* **1999**, *110*, 1856−1872.

AR010026A